AD-A104 022 SRI INTERNATIONAL MENLO PARK CA F/G 20/14
PROPAGATION EFFECTS IN DISTURBED ENVIRONMENTS.(U)
JAN 81 C L RINO DNA001-80-C-0009
UNCLASSIFIED DNA-5637F NL

1 OF 1
AD A
104022

END
DATE
FILMED
10-81
DTIC

AD A104022

DNA 5637F

PROPAGATION EFFECTS IN DISTURBED ENVIRONMENTS

(12)

LEVEL II

Charles L. Rino
SRI International
333 Ravenswood Avenue
Menlo Park, California 94025

1 January 1981

Final Report for Period 30 November 1979—31 December 1980

CONTRACT No. DNA 001-80-C-0009

APPROVED FOR PUBLIC RELEASE;
DISTRIBUTION UNLIMITED.

THIS WORK SPONSORED BY THE DEFENSE NUCLEAR AGENCY
UNDER RDT&E RMSS CODE B322080464 S99QAXHB05422 H2590D.

Prepared for
Director
DEFENSE NUCLEAR AGENCY
Washington, D. C. 20305

Destroy this report when it is no longer needed. Do not return to sender.

PLEASE NOTIFY THE DEFENSE NUCLEAR AGENCY, ATTN: STTI, WASHINGTON, D.C. 20305, IF YOUR ADDRESS IS INCORRECT, IF YOU WISH TO BE DELETED FROM THE DISTRIBUTION LIST, OR IF THE ADDRESSEE IS NO LONGER EMPLOYED BY YOUR ORGANIZATION.

UNCLASSIFIED

SECURITY CLASSIFICATION OF THIS PAGE (When Data Entered)

REPORT DOCUMENTATION PAGE

READ INSTRUCTIONS BEFORE COMPLETING FORM

1. REPORT NUMBER: DNA 5637F	2. GOVT ACCESSION NO.: AD-A104 022
3. RECIPIENT'S CATALOG NUMBER	
4. TITLE (and Subtitle): PROPAGATION EFFECTS IN DISTURBED ENVIRONMENTS	5. TYPE OF REPORT & PERIOD COVERED: Final Report for the Period 30 Nov 79-31 Dec 80
	6. PERFORMING ORG. REPORT NUMBER: SRI Project 1129
7. AUTHOR(s): Charles L. Rino	8. CONTRACT OR GRANT NUMBER(s): DNA 001-80-C-0009
9. PERFORMING ORGANIZATION NAME AND ADDRESS: SRI International, 333 Ravenswood Avenue, Menlo Park, California 94025	10. PROGRAM ELEMENT, PROJECT, TASK AREA & WORK UNIT NUMBERS: Subtask S99QAXHB054-22
11. CONTROLLING OFFICE NAME AND ADDRESS: Director, Defense Nuclear Agency, Washington, D.C. 20305	12. REPORT DATE: 1 January 1981
	13. NUMBER OF PAGES: 38
14. MONITORING AGENCY NAME & ADDRESS (if different from Controlling Office)	15. SECURITY CLASS (of this report): UNCLASSIFIED
	15a. DECLASSIFICATION/DOWNGRADING SCHEDULE: N/A

16. DISTRIBUTION STATEMENT (of this Report)

Approved for public release; distribution unlimited.

17. DISTRIBUTION STATEMENT (of the abstract entered in Block 20, if different from Report)

18. SUPPLEMENTARY NOTES

This work was sponsored by the Defense Nuclear Agency under RDT&E RMSS Code B322080464 S99QAXHB05422 H2590D.

19. KEY WORDS (Continue on reverse side if necessary and identify by block number)

Scintillation
Striations
Radio-wave Propagation

20. ABSTRACT (Continue on reverse side if necessary and identify by block number)

Radio beacon diagnostics are still the least expensive means of obtaining data on naturally occurring and artificially induced striations. To exploit this capability fully, we develop the theory for interpreting rocket-beacon data when the velocity component along the line of sight to the receiver is much larger than the transverse component. A simple and direct relationship is shown to exist between the beacon-phase spectrum and the one-dimensional in-situ spectrum that does not involve any unknown parameters, such as the path length within the disturbance.

DD FORM 1 JAN 73 1473 EDITION OF 1 NOV 65 IS OBSOLETE

UNCLASSIFIED

SECURITY CLASSIFICATION OF THIS PAGE (When Data Entered)

410281

A model is also developed for computing the Doppler spectrum for the usual situation in which the transverse velocity component dominates.

TABLE OF CONTENTS

LIST OF ILLUSTRATIONS

I INTRODUCTION

Theoretical work in wave propagation in randomly irregular media has progressed considerably over the last several years [Flatté et al., 1980; Rino et al., 1980b; Rino, 1980]. A collection of comparatively simple formulas has emerged that characterize the most important channel effects--temporal coherence loss, frequency coherence loss, and angle scattering,--under conditions of strong scattering, such as would occur in the ionosphere following a high-altitude nuclear detonation. To the extent that these results have been tested, they have proven accurate.

Insofar as basic, theoretical work on propagation is concerned little more is required for predicting system performance in highly disturbed, but known propagation environments. The basic problem of accurately characterizing such propagation environments remains, however, and new issues continue to emerge. For example, in the power-law environments that seem characteristic of all turbulent channels, the severity of the propagation effects are sensitive to changes in the spectral index. To study such subtle effects, a refined propagation theory is important because "channel sounding" remains the most economical means of obtaining data on irregularity structures. Under this contract, we have investigated a new technique for beacon diagnostics.

For some time there has been concern about the accuracy with which the scintillation structure "mirrors" the underlying irregularity structure that causes the scintillation. This concern was intensified when the Wideband satellite data showed a spectral index that was not only shallower than was expected, but also variable. This dilemma has only recently been resolved by carefully analyzing data from the Atmospheric Explorer Satellite E (AE-E)[Livingston et al., 1980]. These data showed that the in-situ spectral index is indeed more

shallowly sloped than expected and that it varies systematically, as the Wideband satellite data implied.

In addition to the shape of the spectral density function (SDF), we would like to measure the absolute electron-density fluctuation level or turbulent strength (as distinct from $\Delta N/N$) for each spectral component. To do so from conventional phase-scintillation data involves a two-fold complication:

(1) The level of phase-scintillation depends on the propagation geometry relative to the principal irregularity axis of elongation and the corresponding "stretch" factors or axial ration.

(2) The level of phase-scintillation depends on the integral along the propagation path.

Because the irregularity anisotrophy, the path length of, and, in particular, the structure variation along the propagation path are a priori unknown, a completely unambiguous determination of turbulent strength from such scintillation data is not feasible.

In the DNA PLUMEX experiment conducted at Kwajalein during July-August 1979, however, a downward-looking radio beacon was flown together with a sophisticated complement of in-situ probes. Unlike the satellite-beacon measurements, in the rocket configuration the velocity component along the line of sight is much larger than the transverse component. A comparative analysis of the in-situ probe and beacon data from PLUMEX has shown that there is a simple derivative relationship between the beacon phase and the in-situ density that does not involve any unknown parameters [Rino et al., 1980; Petriceks, 1980]. Thus, the beacon data can be used to determine the turbulent strength.

Because of the comparative simplicity of such rocket-beacon measurements, we have developed a theory (Section II of this report)

for interpreting rocket beacon-phase spectra where $v_{\parallel} >> v_{\perp}$. The results show that as long as $\beta = v_{\perp}/v_{\parallel}$ is less than $\sim$ 40 percent,

$$\Phi_z(\kappa) = r_e^2 \lambda^2 \Phi_1(\kappa)/\kappa^2 \quad ,$$

where $\Phi_z(\kappa)$ is the beacon-phase SDF and $\Phi_1(\kappa)$ is the one-dimensional SDF as measured by the in-situ probe. The relationship obviously breaks down at small wave numbers, but the analysis shows that, depending on β, the relationship holds to within a few spectral resolution cells of the smallest resolvable Fourier component. Because the classical electron radius, r_e, and the wavelength, λ, are known, the beacon-phase SDF can be simply and unambiguously related to the in-situ SDF. The technique is, therefore, potentially useful for future diagnostic rocket probes.

In Section III of this report, we have investigated the simplest form of the mutual coherence function, which is useful for modeling the Doppler spectrum of a scintillating signal. An approximate formula is developed that relates the perturbation strength to the spectral width without having to evaluate gamma functions. Two limiting analytic forms for the Doppler spectrum are derived: one characterizes shallowly-sloped phase spectra and has a power-law form; the second has a Gaussian form and is appropriate for more steeply-sloped spectral-density functions. Numerical computations are presented that show the variation of the spectral shape with changing the spectral index between the two extremes where analytic results can be obtained.

These results are useful for both predictive modeling and data analysis. The Doppler spectral model is being verified concurrently using Wideband satellite data.

II RADIO-BEACON MEASUREMENTS OF LOCAL IRREGULARITY STRUCTURES

A. Background

Over the last decade, extensive phase scintillation data have been obtained from low orbiting and geosynchronous satellites [Crane, 1977; Davis et al., 1975; Rino et al., 1980b]. In such measurements both the signal source and receiver are generally well removed from the disturbed medium. Ignoring diffraction effects and temporal changes in the medium, the instantaneous phase perturbation is given by the formula

$$\phi(t) = kR(t) - r_e\lambda \int_0^{\ell_p} N_e\left(\vec{v}_\perp t,\ \eta\right) d\eta \quad , \tag{1}$$

where $k = 2\pi/\lambda$, $R(t)$ is the range to the satellite, ℓ_p is the length of the propagation path within the disturbed medium, and $N_e(\vec{\rho}, z)$ is the local electron density.

The path length changes with time, but ℓ_p is assumed nearly constant over periods long compared to the time scale for phase changes of interest. If $v_\perp = v_y \hat{a}_y$, the phase SDF takes the form

$$\Phi(f) = r_e^2 \lambda^2 \ell_p \int_{-\infty}^{\infty} \Phi\left(\kappa_x,\ \frac{2\pi f}{v_y},\ 0\right) \frac{d\kappa_x}{2\pi} \quad , \tag{2}$$

where $\Phi(\vec{\kappa}, \kappa_z)$ is the three-dimensional SDF of $N_e(\vec{\rho}, z)$. The corresponding one-dimensional SDF measured by an in-situ probe is

$$\Phi_1(f) = \iint_{-\infty}^{\infty} \Phi\left(\kappa_x,\ \frac{2\pi f}{v_y},\ \kappa_z\right) \frac{d\kappa_x}{2\pi} \frac{d\kappa_y}{2\pi} \quad . \tag{3}$$

It is readily shown [Rino, 1979] that if $\Phi(\vec{\kappa}, \kappa_z) \propto q^{-(2\nu+1)}$, then $\Phi(f) \propto f^{-2\nu}$ and $\Phi_1(f) \propto f^{-(2\nu-1)}$. Thus, if $\nu = 1.5$, then the phase SDF has the power-law form f^{-3}, whereas the one-dimensional in-situ has the power-law form f^{-2}. The difference of unity between the in-situ and phase spectral indices has been verified by comparing spectral measurements derived from Wideband satellite phase data and AE-E in-situ data [Livingston et al., 1980].

For a downward-looking, rocket-borne radio beacon, the signal phase takes the form

$$\phi(t) = k(z_0 + v_z t) - r_e \lambda \int_0^{z_0+v_z t} N_e(\vec{v}_\perp t, \eta) d\eta \quad , \tag{4}$$

where v_z and $\vec{v}_\perp$ are the relative velocity components along and transverse to the line of sight to the receiver. The fixed path length z_0 effectively establishes the initial condition for the indefinite integral that $v_z t$ maps out.

In the early development of guided missiles, radio-beacon measurements were used for trajectory evaluation. As with satellite radio navigation, the ionospheric contribution was a source of error. As the techniques were refined, however, the radio-beacon data came to be used to determine ionospheric density profiles [Berning, 1951]. If $v_\perp$ is small, we have only to remove the geometric Doppler term $kv_z t$ in Eq. (4) and differentiate the residual to obtain $N_e(z)$. Note that the measurement gives absolute electron density because only phase changes are involved.

More recently, the technique has been exploited to measure small-scale irregularity structure. In July 1979, a rocket-borne radio beacon was launched from Roi Namur Island in the Kwajalein Atoll into a highly disturbed equatorial ionosphere. The results

of the beacon and probe structure comparisons are described in Rino et al. [1980c]. The data interpretation was based on the assumption that $v_\perp$ in Eq. (4) could be disregarded. This assumption was justified ex post facto by the agreement between the in-situ and beacon data.

In this section we develop the theory, in detail, to assess the general applicability of the radio-beacon measurement technique for determining local in-situ irregularity structures. We begin by computing the general relation between the beacon-phase SDF and $\Phi(\vec{\kappa}, \kappa_z)$.

B. Spectral Relations for Rocket-Beacon Phase Measurements

To simplify notation, we let $z = v_z t$ and consider the indefinite integral

$$N_T(z) = \int_0^{z_0+z} N_e(\vec{\beta} z, \eta)\, d\eta \quad , \tag{5}$$

where

$$\vec{\beta} = \vec{v}_\perp / v_z \quad . \tag{6}$$

If we assume that $N_e(\vec{\rho}, z)$ can be modeled by a statistically homogeneous random process throughout the measurement region, we can write

$$N_e(\vec{\rho}, z) = \iiint \exp\left\{-i(\vec{\kappa} \cdot \vec{\rho} + \kappa_z z)\right\} d\xi_N(\vec{\kappa}, \kappa_z) \quad , \tag{7}$$

where

$$\langle d\xi_N(\vec{\kappa}, \kappa_z)\, d\xi_N^*(\vec{\kappa}', \kappa_z')\rangle = \frac{1}{(2\pi)^3}\, \Phi(\vec{\kappa}, \kappa_z)\,\delta(\vec{\kappa} - \vec{\kappa}')\,\delta(\kappa_z - \kappa_z') \qquad (8)$$

is a purely formal definition of the orthogonal increments property of the Fourier spectrum $d\xi_N(\vec{\kappa}, \kappa_z)$.

By substituting Eq. (7) into Eq. (5) and changing the order of integration, we can eliminate the indefinite integral in Eq. (5). The result is

$$N_T(z) = \iiint \exp\left\{-i\vec{\kappa}\cdot\vec{\rho}_z\right\} \left[\frac{\exp\{-i\kappa_z(z + z_0)\}-1}{-i\kappa_z}\right] d\xi_N(\vec{\kappa}, \kappa_z) \quad . \qquad (9)$$

Because we can only compute the finite Fourier transform, we shall only consider the integral

$$\hat{N}_T(\kappa_z) = \int_0^L N_T(z)\exp\left\{i\kappa_z z\right\} dz \quad . \qquad (10)$$

In fact, $N_T(z)$ must be modified to avoid contamination of the spectral estimate because of "end point mismatch." Such subtleties need not be formally carried through the analysis, however.

If Eq. (9) is now substituted into Eq. (10) and the integration over z performed, the result is

$$\hat{N}_T(\kappa_z) = \iiint \exp\{-i\kappa_z' z_0\}\, (\vec{\kappa}'\cdot\vec{\rho}, \kappa_z', \kappa_z; z_0)\, \frac{d\xi_N(\vec{\kappa}'; \kappa_z')}{\kappa_z'} \quad . \qquad (11)$$

where

$$D_L(q_1, q_2, q_3; z_0) \triangleq \left[\frac{\exp\left\{-i(q_1 + q_2 - q_3)L\right\} - 1}{(q_1 + q_2 - q_3)} - \exp\left\{iq_2 z_0\right\} \right.$$

$$\left. \times \frac{\exp\left\{-i(q_1 - q_3)L\right\} - 1}{(q_1 - q_3)} \right] \quad . \tag{12}$$

An estimate of the SDF of $N_T(z)$ is obtained by computing $|\hat{N}_T(\kappa_z)|^2/L$ and averaging to smooth the statistical fluctuations. The result is close to the expectation value,

$$\hat{\Phi}_z(\kappa_z) \doteq \langle|\hat{N}_T(\kappa_z)|^2\rangle/L \quad . \tag{13}$$

To evaluate Eq. (13), we substitute $\hat{N}_T(\kappa_z)$ from Eq. (11) and use the orthogonal increments property Eq. (8) to obtain

$$\hat{\Phi}_z(\kappa_z) = \iiint_{-\infty}^{\infty} \frac{1}{L} \left|D_L(\vec{\kappa}'\cdot\vec{\beta}, \kappa_z', \kappa_z; z_0)\right|^2 \frac{\Phi(\kappa', \kappa_z')}{\kappa_z'^2} \frac{d\kappa'}{(2\pi)^2} \frac{d\kappa_z'}{2\pi} \quad . \tag{14}$$

We note that there is no singularity at $\kappa_z' = 0$ because

$$\lim_{\kappa_z' \to 0} D_L(\vec{\kappa}'\cdot\vec{\beta}, \kappa_z', \kappa_z; z_0)\kappa_z'^{-2} = \frac{\sin^2[(\vec{\kappa}'\cdot\vec{\beta} - \kappa_z)L/2]}{(\vec{\kappa}'\cdot\vec{\beta} - \kappa_z)^2} \quad . \tag{15}$$

Let us first consider the special case for which $\beta = 0$. Then,

$$\hat{\Phi}_z(\kappa_z) = \int_{-\infty}^{\infty} \frac{1}{L} \left| D_L(0, \kappa_z', \kappa_z; z_0) \right|^2 \frac{\Phi_1(\kappa_z')}{\kappa_z'^2} \frac{d\kappa_z'}{2\pi} \quad , \tag{16}$$

where

$$\Phi_1(\kappa_z) = \iint_{-\infty}^{\infty} \Phi(\vec{\kappa}, \kappa_z) \frac{d\vec{\kappa}}{(2\pi)^2} \tag{17}$$

is the one-dimensional spatial SDF derived from a probe scanning along the z axis which should not be confused with the temporal SDF defined by Eq. (3).

The general behavior of Eq. (16) is readily established. We first isolate the κ_z' regime where Eq. (15) applies. It is sufficient to take $\kappa_z' < 2\pi/L$, whereby

$$\int_{|\kappa_z'|<2\pi/L} \frac{1}{L} \left| D_L(0, \kappa_z', \kappa_z; z_0) \right|^2 \frac{\Phi_1(\kappa_z')}{\kappa_z'^2} \frac{d\kappa_z'}{2\pi}$$

$$< \frac{\sin^2[\kappa_z L/2]}{\kappa_z^2 L} \int_{|\kappa_z'|<\frac{2\pi}{L}} \Phi_1(\kappa_z') \frac{d\kappa_z'}{2\pi} \quad . \tag{18}$$

This contribution to Eq. (16) becomes vanishingly small as κ_z increases; however, for large κ_z

$$\frac{1}{L}\left|D_L(0,\ \kappa_z',\ \kappa_z;\ z_0)\right|^2 \cong \frac{\sin^2\left[(\kappa_z - \kappa_z')\ \frac{L}{2}\right]}{(\kappa_z - \kappa_z')^2 L} \quad . \tag{19}$$

Now, as long as the variation of $\Phi_1(\kappa_z')$ is small over κ_z' intervals, comparable to $2\pi/L$, we can show that

$$\int_{|\kappa_z'|>2\pi/L} \frac{\sin^2\left[(\kappa_z - \kappa_z')\ \frac{L}{2}\right]}{(\kappa_z - \kappa_z')^2 L}\ \frac{\Phi_1(\kappa_z')}{\kappa_z'^2}\ \frac{d\kappa_z'}{2\pi} \cong \frac{\Phi_1(\kappa_z)}{\kappa_z^2} \tag{20}$$

[<u>Rosenblatt</u>, pp. 169-180, 1962], which is sometimes referred to as the "sifting property" of sinc^2.

As long as $\kappa_z > 2\pi/L$, the $\beta = 0$ behavior of Eq. (14) is summarized by

$$\hat{\Phi}_z(\kappa_z) \cong \Phi_1(\kappa_z)/\kappa_z^2 \quad . \tag{21}$$

The relationship Eq. (21) is useful because it involves no unknown paramters, e.g., the length of the propagation path or the axial ratios, which characterize the anisotropy of the medium.

At the opposite extreme where β is very large, we can disregard q_2 in Eq. (12) where is appears next to q_1. The result is

$$\hat{\Phi}_z(\kappa_z) \cong \iint_{-\infty}^{\infty} \frac{\sin^2\left[(\vec{\kappa}'\cdot\vec{\beta} - \kappa_z)L/2\right]}{(\vec{\kappa}'\cdot\vec{\beta} - \kappa_z)2L}$$

$$\times \int_{-\infty}^{\infty} \frac{\sin^2\left[\kappa_z' z_0/2\right]}{\kappa_z'^2} \Phi(\vec{\kappa}', \kappa_z') \frac{d\kappa_z'}{2\pi} \frac{d\vec{\kappa}'}{(2\pi)^2} \quad . \tag{22}$$

In the usual approximation the integral over κ_z' is replaced by $z_0\Phi(\vec{\kappa}'; 0)$. Finally, by letting $\vec{\beta} = \beta\hat{a}_y$ and applying the sifting property of sinc^2 to the κ_y integration, we have

$$\Phi_z(\kappa_z) \cong z_0 \int_{-\infty}^{\infty} \Phi(\kappa_x, \beta\kappa_z, 0) \frac{d\kappa_x}{2\pi} \quad , \tag{23}$$

which is essentially equivalent to Eq. (2). Note that z_0 in Eq. (23) is the distance from the point where the disturbance starts and is, therefore, unknown.

For $0 < \beta << 1$, which is the case of primary interest, we first isolate the region near $\kappa_z' = 0$ and use Eq. (15). In place of Eq. (18) we now have

$$\iiint_{-\infty}^{\infty}\limits_{|\kappa_z'|<2\pi/L} [\qquad] \frac{d\vec{\kappa}}{(2\pi)^2}\frac{d\kappa_z'}{2\pi} \gtrsim \iint_{-\infty}^{\infty} \frac{\sin^2\left[(\vec{\kappa}\cdot\vec{\beta}' - \kappa_z)L/2\right]}{(\vec{\kappa}\cdot\vec{\beta} - \kappa_z)2L}$$

$$\int_{|\kappa_z'|<2\pi/L} \Phi(\vec{\kappa}', \kappa_z') \frac{d\vec{\kappa}'}{(2\pi)^2}\frac{d\kappa_z'}{2\pi} \quad . \tag{24}$$

If we let $\vec{\beta} = \beta\hat{a}_y$ and using the sifting property of sinc^2, the right-hand side of Eq. (24) can be replaced by

$$\iint_{-\infty}^{\infty}\limits_{|\kappa_z'|<2\pi/L} \frac{1}{\beta}\,\Phi(\kappa_x', \kappa_z/\beta, \kappa_z') \frac{d\kappa_x'}{2\pi}\frac{d\kappa_z'}{2\pi} \quad . \tag{25}$$

For a power-law SDF this contribution again decreases rapidly with increasing κ_z.

The behavior of Eq. (14) for the region outside $|\kappa_z'|<2\pi/L$ can be determined with the aid of Figure 1 where the $\kappa_y' - \kappa_z'$ plane has been partitioned into two regions separated by the line $\kappa_y' = \kappa_z'/\beta$. To the right of this line,

$$\frac{1}{L}\,|D_L(\vec{\kappa}'\cdot\vec{\beta}, \kappa_z', \kappa_z; 0)|^2 \cong \frac{\sin^2\left[(\vec{\kappa}'\cdot\vec{\beta} + \kappa_z' - \kappa_z)L/2\right]}{(\vec{\kappa}'\cdot\vec{\beta} + \kappa_z' - \kappa_z)2L} \quad . \tag{26}$$

The lines where Eq. (26) achieves its maximum value are also shown in Figure 1. This behavior is illustrated in the perspective plots of $\frac{1}{L}\left|D_L(\kappa_y'\beta, \kappa_z', \kappa_z; 0)\right|^2$ shown in Figures 2 and 3. For convenience, L was set equal to 2. Figure 2 corresponds to a large κ_z value so that the shaded region $\kappa_y' < \kappa_z'/\beta$ is not entered over the κ_y' range plotted.

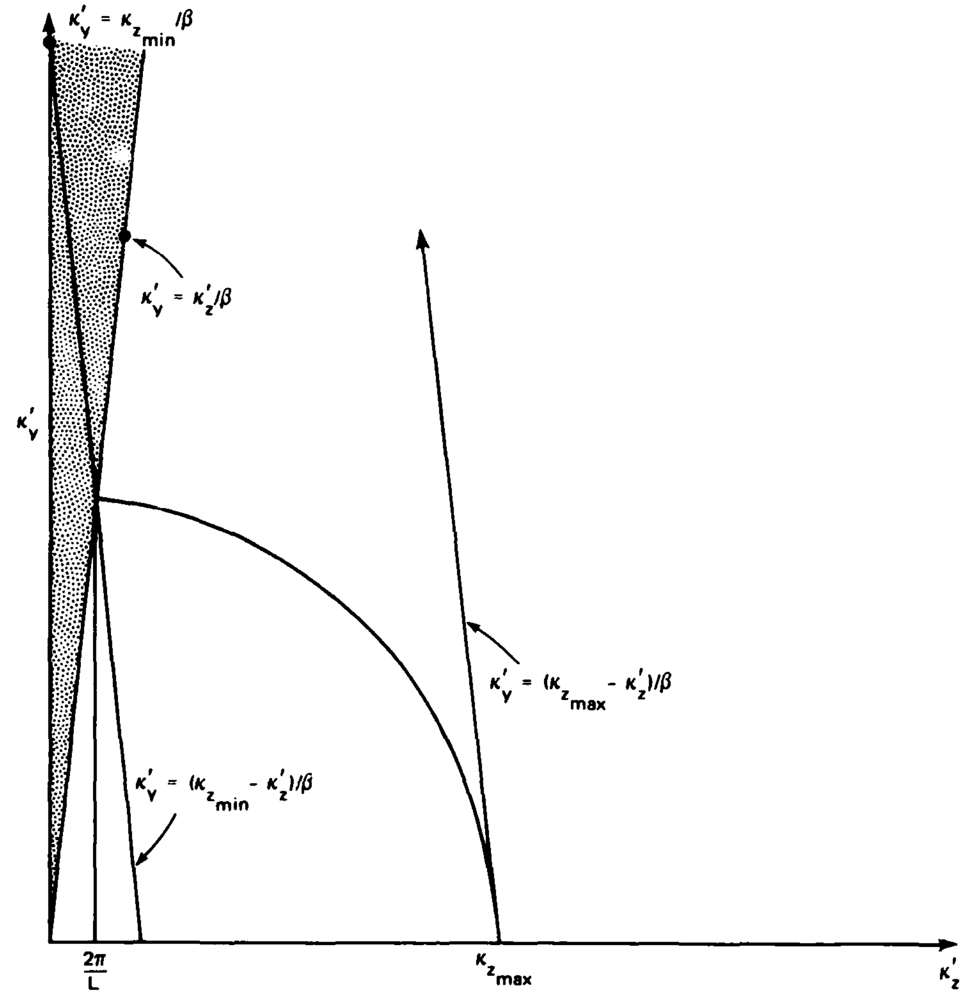

FIGURE 1 REGION OF κ_y' - κ_z' PLANE WHERE $1/L|D_L|$ CAN BE APPROXIMATED BY sinc^2

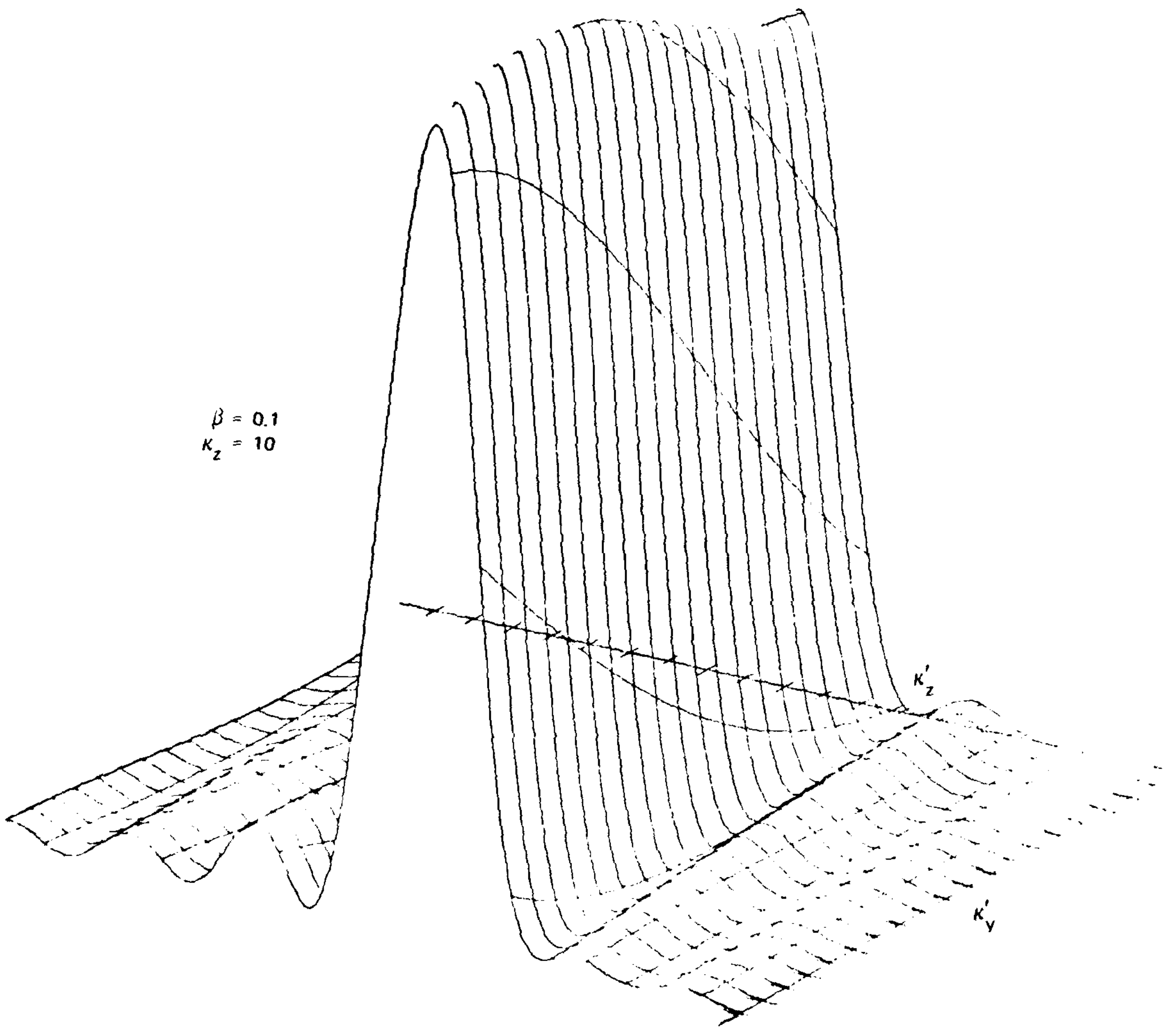

FIGURE 2 PERSPECTIVE PLOT SHOWING $1/L|D_L|^2$ AS A FUNCTION OF κ_y' AND κ_z' FOR SMALL β AND LARGE κ_z

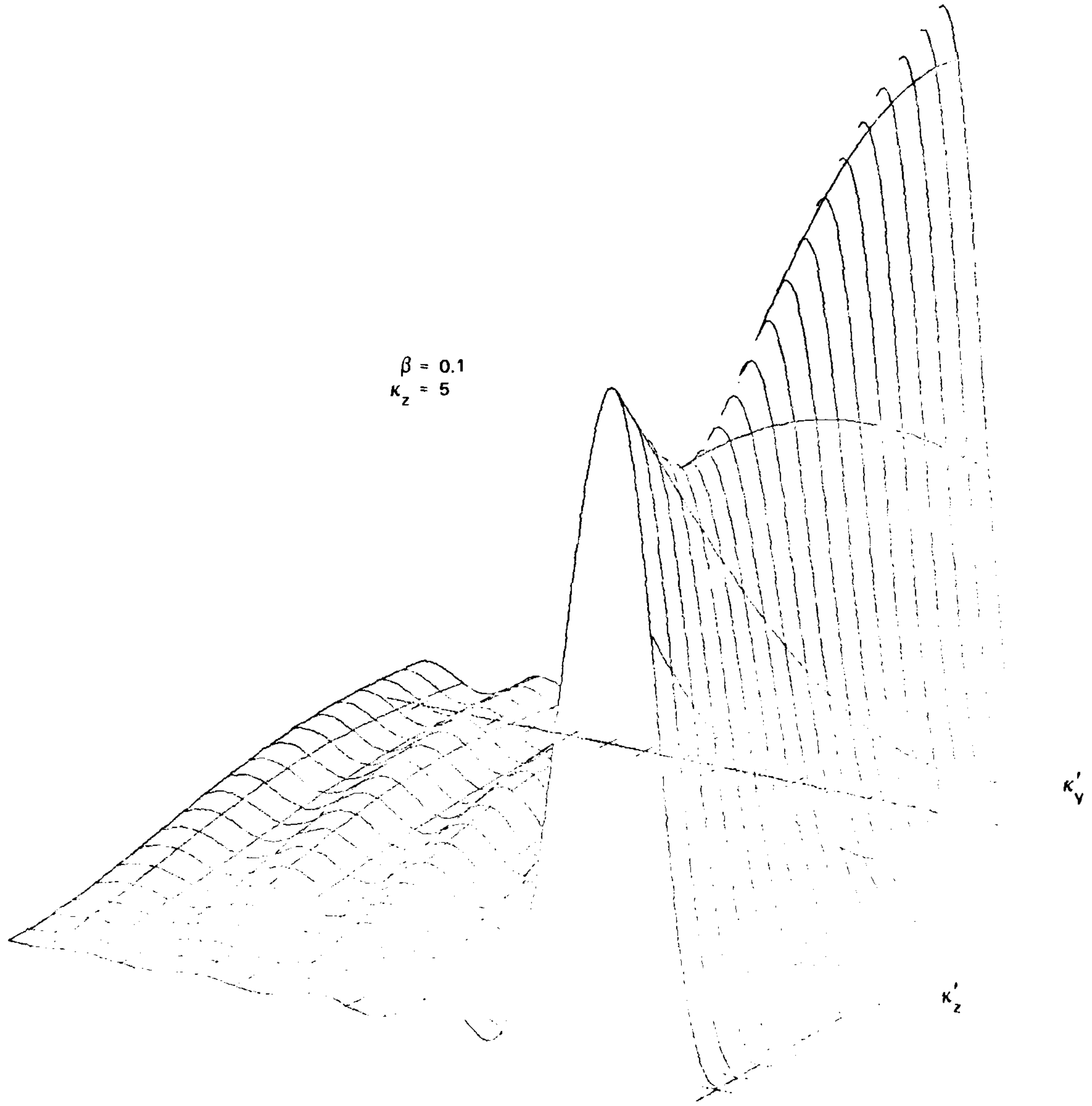

FIGURE 3 PERSPECTIVE PLOT SHOWING THE EFFECT OF DECREASING κ_z

In Figure 3, the region where Eq. (26) breaks down is evident. The effect of increasing β is shown in Figure 4.

We have already established that the contribution to Eq. (14) for small κ_z' is negligible when $\kappa_z << 2\pi/L$. Thus, there is a minimum value of κ_z as shown in Figure 1. Beyond an arc drawn from the intersection of $\kappa_z' = 2\pi/L$ and $\kappa_y' = (\kappa_{z_{min}} - \kappa_z')/\beta$, the contribution to Eq. (14) of $\Phi(\vec{\kappa}; \kappa_z')/\kappa_z'^2$ must be negligible. We can then apply the sifting property of Eq. (26) to obtain

$$\hat{\Phi}_z(\kappa_z) \cong \iint \frac{\Phi(\vec{\kappa}'; \kappa_z - \vec{\kappa}'\cdot\vec{\beta})}{(\kappa_z - \vec{\kappa}'\cdot\beta)^2} \frac{d\vec{\kappa}'}{(2\pi)^2} \cong \Phi_1(\kappa_z)/\kappa_z^2 \quad . \tag{27}$$

The second approximation applied because $\kappa_z << \vec{\kappa}' \cdot \vec{\beta}$ in the region where Eq. (26) is valid. For a typical power-law SDF, the validity conditions for Eq. (27) are easily achieved $\beta < \cdot 4$.

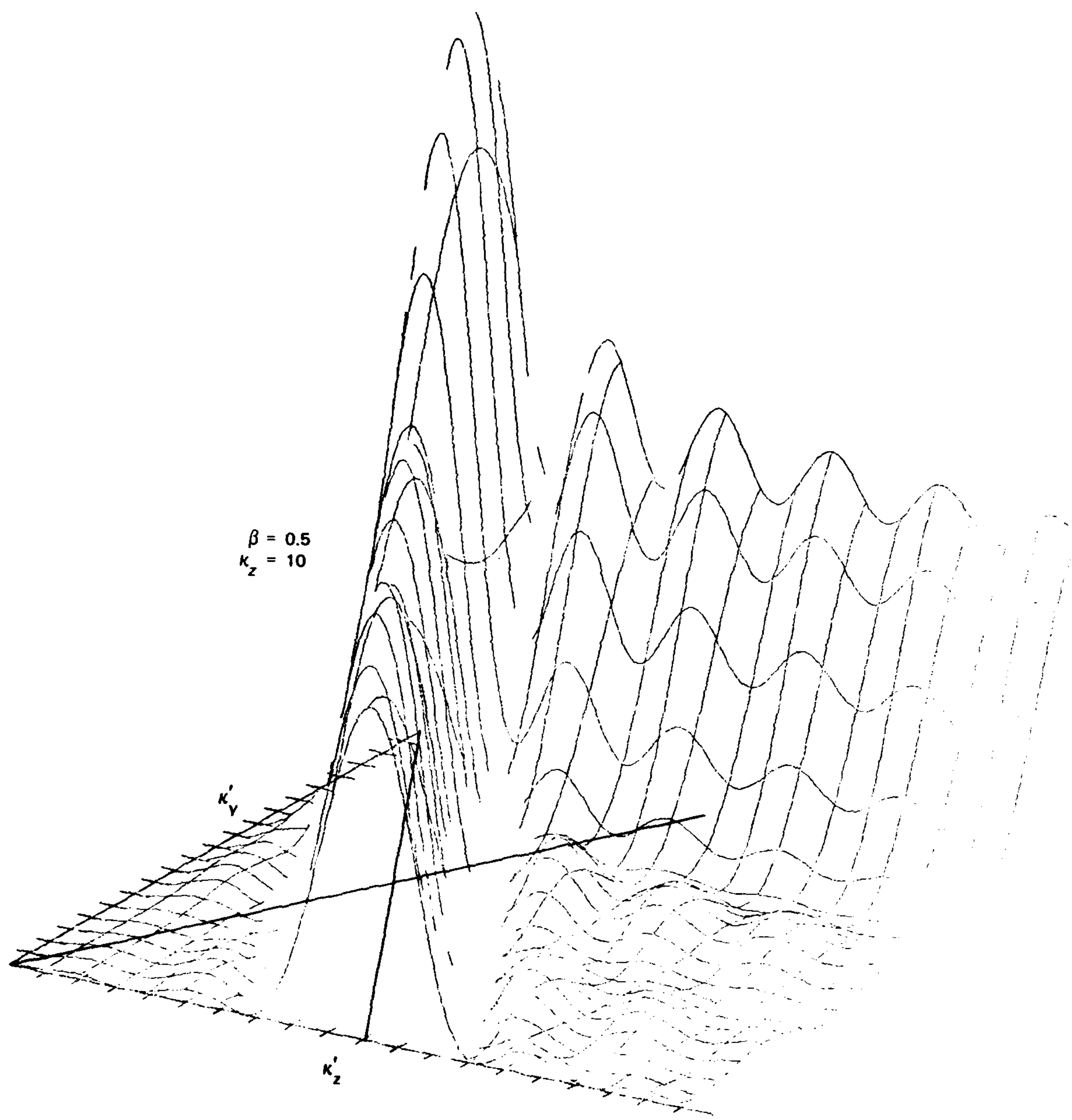

FIGURE 4 PERSPECTIVE PLOT SHOWING THE EFFECT OF INCREASING β

III DOPPLER SPECTRUM

A. Background

For some predictive scintillation codes, it is useful to model the Doppler spectrum of the complex signal, v(t). The Doppler spectrum is formally the Fourier transform of the mutual coherence function

$$R_v(\tau) = \langle v(t)v^*(t + \tau)\rangle \quad . \tag{28}$$

Under reasonable assumptions, moreover, $R_v(\tau)$ admits the simple representation

$$R_v(\tau) = \exp\left\{- \frac{1}{2} D_{\delta\phi}(v_{eff}\tau)\right\} \quad , \tag{29}$$

where

$$D_{\delta\phi}(y) = 2\sigma_{\delta\phi}^{\;2} \left[1 - \rho_{\delta\phi}(y)\right] \tag{30}$$

is the phase structure function, $\sigma_{\delta\phi}$ is the rms phase, and $\rho_{\delta\phi}(y)$ is the normalized phase autocorrelation function [$\rho_{\delta\phi}(0) = 1$]. Equation (29) is strictly valid only in the plane normal to the propagation direction, that is, when parallel propagation effects are negligible. The correction factor that must be applied to accommodate parallel propagation effects are described in Rino, Section V, [1980]; thus, we shall only consider Eq. (29) here.

If the three-dimensional spatial SDF of the irregularities has the general power-law form

$$\Phi(\vec{\kappa}, \kappa_z) = \frac{abC_s}{\left[q_0^2 + q^2\right]^{\nu+1/2}} \quad , \tag{31}$$

then $\rho_{\delta\phi}(y)$, the two-dimensional Fourier transform of Eq. (31), can be evaluated as

$$\rho_{\delta\phi}(y) = \frac{2}{\Gamma(\nu - 1/2)} \left|\frac{q_0 y}{2}\right|^{\nu-1/2} K_{\nu-1/2}(q_0 y) \quad , \tag{32}$$

where y is a quadratic form in the spatial separation coordinates, Δ_x and Δ_y, as described in Rino [1979a, b]. However, in spite of the comparatively simple form of Eq. (32), it is too cumbersome for direct use in Eq. (29), and we seek simpler approximate forms.

The simplest approximation that retains a dependence on the spectral index parameter, ν, is

$$D_{\delta\phi}(y) \cong C_{\delta\phi}^{2}\, y^{2\nu-1} \quad , \tag{33}$$

where $C_{\delta\phi}^2$ is the phase structure constant

$$C_{\delta\phi}^{2} = r_e^{2} \lambda^{2} \ell_p \frac{C_{\delta\phi}}{2\pi} \frac{2\Gamma(1.5 - \nu)}{\Gamma(0.5 + \nu)(2\nu - 1)2^{2\nu-1}} \quad , \tag{34}$$

which is valid for $\nu < 1.5$. Equation (33) is obtained as an asymptotic approximation Eq. (30) in the limit as q_0 becomes very small [Rino, 1979b]. Note that Eq. (33) does not retain an explicit dependence on q_0.

For more steeply sloped spectra ($\nu > 1.5$), a quadratic approximation of the form

$$D_{\delta\phi}(y) \cong D_1 y^2 \tag{35}$$

is admissible. In Eq. (35), D_1 is the first nonzero coefficient in a Taylor series expansion of $D_{\delta\phi}(y)$. The expansion coefficients generally do not exist independently from an inner-scale cut-off, [Rino et al., 1980], although D_1 is independent of q_0 and q_i for $\nu > 1.5$.

For the entire range of ν values, $R_v(\tau)$ admits the approximate form

$$R_v(\tau) = \exp\left\{- 1/2\ C_{\delta\phi}{}^2\ |y|^{\min(2\nu-1,2)}\right\} , \tag{36}$$

where

$$\frac{2\pi C_{\delta\phi}{}^2}{C_p} = \begin{cases} \dfrac{2(1.5 - \nu)}{\Gamma(0.5 + \nu)(2\nu - 1)\nu^{2\nu-1}} & 0.5 < \nu < 1.5 \\[2ex] - \frac{1}{2} \log(q_i/q_0 & \nu = 1.5 \\[2ex] \dfrac{\Gamma(\nu - 1.5)}{4\Gamma(\nu - 0.5)} & \nu > 1.5 \end{cases} \tag{37}$$

A plot of $2\pi C_{\delta\phi}{}^2/C_p$ as a function of ν is illustrated in Figure 5. The singular behavior at $\nu = 1.5$ is indicative of a breakdown in both the asymptotic and quadratic approximations. The dashed line is probably closer to the correct functional dependence of an asymptotic approximation of the form of Eq. (32).

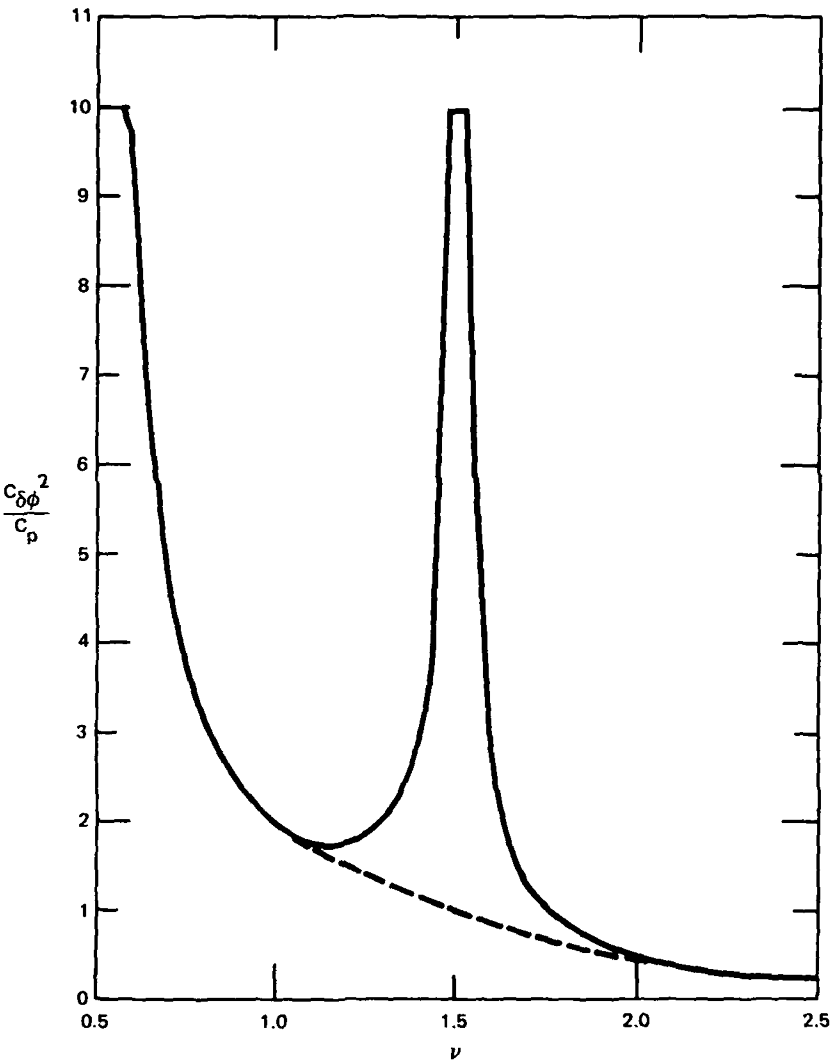

FIGURE 5 VARIATION OF STRUCTURE FUNCTION EXPANSION COEFFICIENT WITH CHANGING SPECTRAL INDEX

For predictive modeling, therefore, it is convenient to take

$$2\nu C_{\delta}^{2}/C_{p} \cong \nu^{2} - 4.5\nu + 5.5 \quad 1.0 \leq \nu \leq 2.0 \quad , \tag{38}$$

which follows the dashed curve in Figure 5 very closely. Approximations such as Eq. (38), are particularly convenient because of the evidence that the spectral index itself varies systematically with changing turbulent strength [Livingston et al., 1980; Rino et al., 1980c]. In any case, for our purposes here, we are only interested in the behavior of Eq. (36) as a function of ν. Because of the simple power-law form of the argument of the exponential function, C_{δ}^{2} is effectively only a scale factor.

B. Special Cases and Numerical Computations

To compute the Doppler spectrum, we must evaluate the integral

$$\Phi(f) = \int_{-\infty}^{\infty} R_{v}(\tau)\ \exp\left\{-2\pi i f\tau\right\} d\tau \quad . \tag{39}$$

Substituting $y = v_{eff}\tau$ into Eq. (36) gives

$$R_{v}(\tau) = \exp\left\{-\left|\frac{\tau}{\tau_{0}}\right|^{\min(2\nu-1,2)}\right\} \quad . \tag{40}$$

where

$$\tau_{0} = \frac{1}{v_{eff}}\left(\frac{2}{C_{\delta}^{2}}\right)^{\frac{1}{\min(2\nu-1,2)}} \quad . \tag{41}$$

If ν = 1, Eq. (39) admits the exact solution

$$\Phi(f) = \frac{1}{\tau_0} \frac{2}{1 + (2\pi\tau_0 f)^2} \quad . \tag{42}$$

Similarly, if ν = 1.5, then $\Phi(f)$ takes the Gaussian form

$$\Phi(f) = \frac{\sqrt{\pi}}{\tau_0} \exp\left\{ - \frac{(2\pi\tau_0 f)^2}{4} \right\} \quad . \tag{43}$$

Thus, the general trend is from shallow power-law to Gaussian as ν increases.

This is verified in the numerical evaluations of Eq. (39) using the fast Fourier transform algorithm. In Figure 6, $\tau_0\Phi(f)$ is plotted for ν = 0.8, ν = 0.9, and ν = 1.0. For such shallowly sloped phase spectra, the overall shape of $\Phi(f)$ changes little. As the slope increases, however, shape changes rapidly--as shown in Figure 7 where $\tau_0\Phi(f)$ is plotted for ν = 1.3, ν = 1.4, and ν = 1.5.

For predictive modeling, therefore, we can use Eq. (42), where the spectral index is comparatively small, and Eq. (43) for the opposite extreme. It should be kept in mind, however, that τ_0 itself depends on the spectral index parameter, ν, as well as on the perturbation strength.

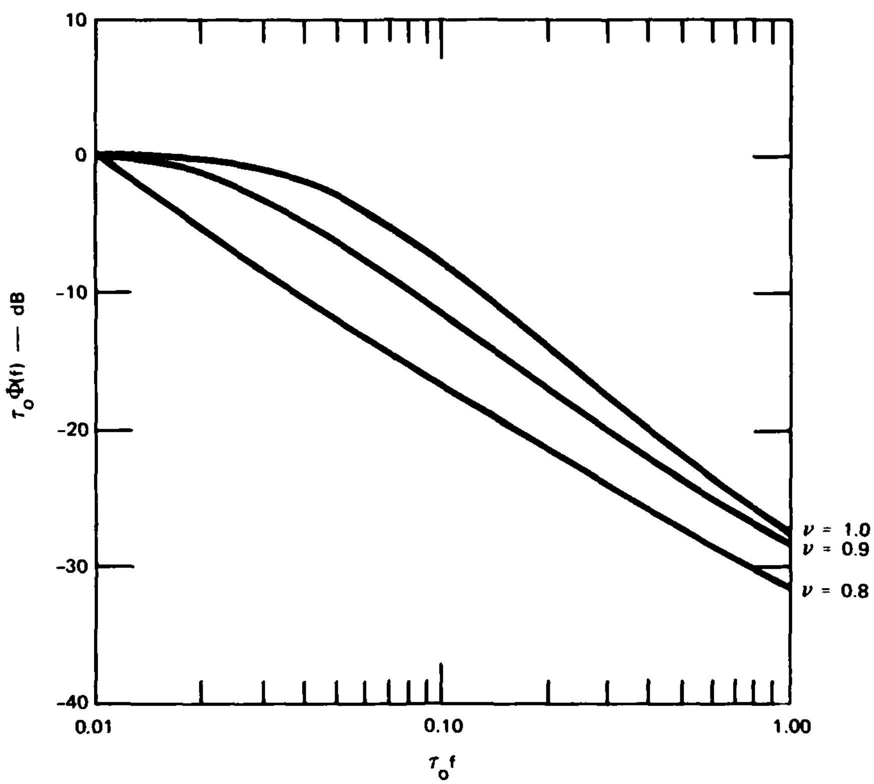

FIGURE 6 DOPPLER SPECTRUM FOR SHALLOWLY SLOPED PHASE SPECTRA

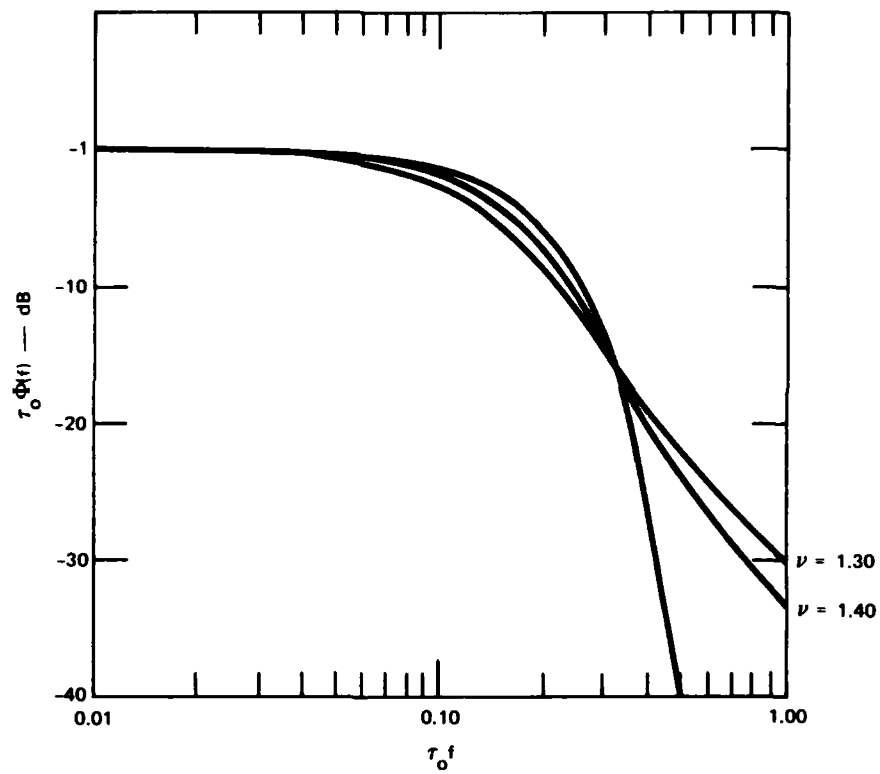

FIGURE 7 DOPPLER SPECTRUM FOR MORE STEEPLY SLOPED PHASE SPECTRA

IV CONCLUSIONS

In this report we developed a theory to interpret beacon-phase data when the line-of-sight velocity component is much larger than the transverse component. In that situation, there is a simple relationship between the phase spectral-density function and the one-dimensional in-situ spectral-density function that a rocket-borne density probe would be measured. Thus, both the spectral shape and the turbulent strength can be determined.

Because the rocket beacon signal itself is the data source, no telemetry is required. Thus, such beacon measurements provide a comparatively inexpensive means for obtaining quantative ionospheric structure measurements.

Also, a simple mathematical model was developed for predicting the Doppler spectrum of a satellite signal received in the usual situation in which the transverse Doppler component dominates. This model is useful both for data interpretation and system analysis.

Most other theoretical results of interest have been verified. The mutual coherence function model itself, which is the starting point for the Doppler spectrum computations, has not yet been tested against real data, but this effort is being pursued under a separate contract.

REFERENCES

Berning, W. W., "Charge Densities in the Ionosphere from Radio Doppler Data," J. of Meteor., Vol. 8, p. 176 (1951).

Crane, R., "Ionospheric Scintillation," Proc. IEEE, Vol. 65, No. 2, p. 180 (1977).

Davies, K., R. B. Fritz, R. N. Grubb, and J. E. Jones, "Some Early Results from the ATS-6 Radio Beacon Experiments," Radio Science, Vol. 10, p. 785 (1975).

Flatte, S. M., R. Dashen, W. H. Munk, and F. Zachariasen, "Sound Transmission Through a Fluctuating Ocean," (Cambridge, 1979).

Livingston, R. C., C. L. Rino, J. P. McClure, and W. B. Hanson, "Spectral Characteristics of Medium-Scale Equatorial F-Region Irregularities," J. Geophys. Res., Accepted for Publication (1980).

Petriceks, J., "Rocket RF-Beacon Experiment for the Summer 1979 Kwajalein Campaign," Proceedings of the Summer Equatorial Experiment Data Review Meeting (March 1980).

Rino, C. L., "A Power-Law Phase Screen Model for Ionospheric Scintillation 1. Weak Scatter," Radio Science, Vol. 14, No. 6, p. 1135 (1979).

Rino, C. L., "A Power-Law Phase Screen Model for Ionospheric Scintillation 2. Strong Scatter," Radio Science, Vol. 14, No. 6, p. 1147 (1979b).

Rino, C. L., "Propagation Modeling and Evaluation of Communication System Performance in Nuclear Environments," DNA 5265F, Final Report, Contract DNA001-77-C-0038, SRI Project 5960, SRI International, Menlo Park, CA. (February 1980).

Rino, C. L., V. H. Gonzales, A. R. Hessing, "Coherence Bandwidth Loss in Transionospheric Radio Propagation," Topical Report, Contract DNA001-80-C-0077, SRI Project 1284, SRI International, Menlo Park, CA. (March 1980a).

Rino, C. L., R. C. Livingston, B. C. Fair, M. D. Cousins, "Continued Performance of the Wideband Satellite Experiment," Final Report, Contract DNA001-77-C-0220, SRI Project 6434, SRI International, Menlo Park, CA. (June 1980b).

Rino, C. L., R. T. Tsunoda, J. Petriceks, R. C. Livingston, M. C. Kelley, and K. D. Baker, "Simultaneous Rocket-Borne Beacon and In-Situ Measurements of Equatorial Spread F--Long Wavelength Results," J. Geophys. Res., Accepted for Publication (1980).

Rosenblatt, M., Random Processes (Oxford Press, N.Y., 1962).

DISTRIBUTION LIST

DEPARTMENT OF DEFENSE

Assistant Secretary of Defense
Comm, Cmd, Cont & Intell
ATTN: Dir of Intelligence Sys, J. Babcock

Assistant to the Secretary of Defense
Atomic Energy
ATTN: Executive Assistant

Command & Control Technical Center
ATTN: C-312, R. Mason
ATTN: C-650, G. Jones
3 cy ATTN: C-650, W. Heidig

Defense Communications Agency
ATTN: Code 480
ATTN: Code 480, F. Dieter
ATTN: Code 810, J. Barna
ATTN: Code 205
ATTN: Code 101B

Defense Communications Engineer Center
ATTN: Code R123
ATTN: Code R410, N. Jones

Defense Intelligence Agency
ATTN: DT-5
ATTN: DB-4C, E. O'Farrell
ATTN: DB, A. Wise
ATTN: DT-1B
ATTN: DIR, E. Tighe
ATTN: DC-7D, W. Wittig

Defense Nuclear Agency
ATTN: NAFD
ATTN: STNA
ATTN: RAEE
ATTN: NATD
3 cy ATTN: RAAE
4 cy ATTN: TITL

Defense Technical Information Center
12 cy ATTN: DD

Field Command
Defense Nuclear Agency
ATTN: FCPR

Field Command
Defense Nuclear Agency
Livermore Branch
ATTN: FCPRL

Interservice Nuclear Weapons School
ATTN: TTV

Joint Chiefs of Staff
ATTN: C3S
ATTN: C3S, Evaluation Office

Joint Strat Tgt Planning Staff
ATTN: JLTW-2
ATTN: JLA

Under Secretary of Def for Rsch & Engrg
ATTN: Strategic & Space Sys (OS)

DEPARTMENT OF DEFENSE (Continued)

National Security Agency
ATTN: W-32, O. Bartlett
ATTN: B-3, F. Leonard
ATTN: R-52, J. Skillman

WWMCCS System Engineering Org
ATTN: R. Crawford

DEPARTMENT OF THE ARMY

Assistant Chief of Staff for Automation & Comm
Department of the Army
ATTN: DAAC-ZT, P. Kenny

Atmospheric Sciences Laboratory
U.S. Army Electronics R&D Command
ATTN: DELAS-EO, F. Niles

BMD Advanced Technology Center
Department of the Army
ATTN: ATC-T, M. Capps
ATTN: ATC-O, W. Davies

BMD Systems Command
Department of the Army
2 cy ATTN: BMDSC-HW

Deputy Chief of Staff for Ops & Plans
Department of the Army
ATTN: DAMO-RQC

Harry Diamond Laboratories
Department of the Army
ATTN: DELHD-I-TL, M. Weiner
ATTN: DELHD-N-P, F. Wimenitz
ATTN: DELHD-N-RB, R. Williams
ATTN: DELHD-N-P

U.S. Army Chemical School
ATTN: ATZN-CM-CS

U.S. Army Comm-Elec Engrg Instal Agency
ATTN: CCC-EMEO-PED, G. Lane
ATTN: CCC-CED-CCO, W. Neuendorf

U.S. Army Communications Command
ATTN: CC-OPS-W
ATTN: CC-OPS-WR, H. Wilson

U.S. Army Communications R&D Command
ATTN: DRDCO-COM-RY, W. Kesselman

U.S. Army Foreign Science & Tech Ctr
ATTN: DRXST-SD

U.S. Army Materiel Dev & Readiness Cmd
ATTN: DRCLDC, J. Bender

U.S. Army Missile Intelligence Agency
ATTN: J. Gamble

U.S. Army Nuclear & Chemical Agency
ATTN: Library

DEPARTMENT OF THE ARMY (Continued)

U.S. Army Satellite Comm Agency
ATTN: Document Control

U.S. Army TRADOC Sys Analysis Actvy
ATTN: ATAA-PL
ATTN: ATAA-TDC
ATTN: ATAA-TCC, F. Payan, Jr

DEPARTMENT OF THE NAVY

COMSPTEVFOR
Department of the Navy
ATTN: Code 605, R. Berg

Joint Cruise Missiles Project Ofc
Department of the Navy
ATTN: JCMG-707

Naval Air Development Center
ATTN: Code 6091, M. Setz

Naval Air Systems Command
ATTN: PMA 271

Naval Electronic Systems Command
ATTN: PME 106-4, S. Kearney
ATTN: PME 117-2013, G. Burnhart
ATTN: PME 117-20
ATTN: Code 3101, T. Hughes
ATTN: Code 501A
ATTN: PME 106-13, T. Griffin
ATTN: PME 117-211, B. Kruger

Naval Intelligence Support Ctr
ATTN: NISC-50

Naval Ocean Systems Center
ATTN: Code 532, J. Bickel
ATTN: Code 5322, M. Paulson
3 cy ATTN: Code 5324, W. Moler
3 cy ATTN: Code 5323, J. Ferguson

Naval Research Laboratory
ATTN: Code 7550, J. Davis
ATTN: Code 4187
ATTN: Code 4780, S. Ossakow
ATTN: Code 7500, B. Wald
ATTN: Code 7950, J. Goodman
ATTN: Code 4700, T. Coffey

Naval Space Surveillance System
ATTN: J. Burton

Naval Surface Weapons Center
ATTN: Code F31

Naval Telecommunications Command
ATTN: Code 341

Office of Naval Research
ATTN: Code 465
ATTN: Code 420
ATTN: Code 421

Office of the Chief of Naval Operations
ATTN: OP 65
ATTN: OP 941D
ATTN: OP 981N

DEPARTMENT OF THE NAVY (Continued)

Strategic Systems Project Office
Department of the Navy
ATTN: NSP-2722, F. Wimberly
ATTN: NSP-2141
ATTN: NSP-43

DEPARTMENT OF THE AIR FORCE

Aerospace Defense Command
Department of the Air Force
ATTN: DC, T. Long

Air Force Geophysics Laboratory
ATTN: OPR, H. Gardiner
ATTN: OPR-1
ATTN: LKB, K. Champion
ATTN: OPR, A. Stair
ATTN: S. Basu
ATTN: PHP
ATTN: PHI, J. Buchau
ATTN: R. Thompson

Air Force Weapons Laboratory
Air Force Systems Command
ATTN: SUL
ATTN: NTYC
ATTN: NTN

Air Force Wright Aeronautical Lab
ATTN: W. Hunt
ATTN: A. Johnson

Air Logistics Command
Department of the Air Force
ATTN: OO-ALC/MM, R. Blackburn

Air University Library
Department of the Air Force
ATTN: AUL-LSE

Air Weather Service, MAC
Department of the Air Force
ATTN: DNXP, R. Babcock

Assistant Chief of Staff
Intelligence
Department of the Air Force
ATTN: INED

Assistant Chief of Staff
Studies & Analyses
Department of the Air Force
ATTN: AF/SASC, W. Keaus
ATTN: AF/SASC, C. Rightmeyer

Ballistic Missile Office
Air Force Systems Command
ATTN: ENSN, J. Allen

Deputy Chief of Staff
Operations Plans and Readiness
Department of the Air Force
ATTN: AFXOKT
ATTN: AFXOKS
ATTN: AFXOXFD
ATTN: AFXOKCD

DEPARTMENT OF THE AIR FORCE (Continued)

Deputy Chief of Staff
Research, Development, & Acq
Department of the Air Force
ATTN: AFRDS
ATTN: AFRDSS
ATTN: AFRDSP

Electronic Systems Division
Department of the Air Force
ATTN: DCKC, J. Clark

Electronic Systems Division
Department of the Air Force
ATTN: XRW, J. Deas

Electronic Systems Division
Department of the Air Force
ATTN: YSM, J. Kobelski
ATTN: YSEA

Foreign Technology Division
Air Force Systems Command
ATTN: TQTD, B. Ballard
ATTN: NIIS, Library

Headquarters Space Division
Air Force Systems Command
ATTN: SKY, C. Kennedy
ATTN: SKA, D. Bolin

Headquarters Space Division
Air Force Systems Command
ATTN: YZJ, W. Mercer

Headquarters Space Division
Air Force Systems Command
ATTN: E. Butt

Rome Air Development Center
Air Force Systems Command
ATTN: OCS, V. Coyne
ATTN: TSLD

Rome Air Development Center
Air Force Systems Command
ATTN: EEP

Strategic Air Command
Department of the Air Force
ATTN: DCXT
ATTN: NRT
ATTN: DCXR, T. Jorgensen
ATTN: DCX
ATTN: XPFS

OTHER GOVERNMENT AGENCIES

Central Intelligence Agency
ATTN: OSWR/NED

Department of Commerce
National Bureau of Standards
ATTN: Sec Ofc for R. Moore

Department of Commerce
National Oceanic & Atmospheric Admin
ATTN: R. Grubb

OTHER GOVERNMENT AGENCIES (Continued)

Institute for Telecommunications Sciences
ATTN: W. Utlaut
ATTN: A. Jean
ATTN: L. Berry

U.S. Coast Guard
Department of Transportation
ATTN: G-DOE-3/TP54, B. Romine

DEPARTMENT OF ENERGY CONTRACTORS

EG&G, Inc
Los Alamos Division
ATTN: J. Colvin
ATTN: D. Wright

Lawrence Livermore National Lab
ATTN: L-389, R. Ott
ATTN: L-31, R. Hager
ATTN: Technical Info Dept Library

Los Alamos National Scientific Lab
ATTN: MS 664, J. Zinn
ATTN: D. Simons
ATTN: P. Keaton
ATTN: D. Westervelt
ATTN: E. Jones
ATTN: R. Taschek
ATTN: MS 670, J. Hopkins

Sandia National Laboratories
Livermore Laboratory
ATTN: B. Murphey
ATTN: T. Cook

Sandia National Lab
ATTN: ORG 1250, W. Brown
ATTN: ORG 4241, T. Wright
ATTN: Space Project Div
ATTN: 3141
ATTN: D. Thornbrough
ATTN: D. Dahlgren

DEPARTMENT OF DEFENSE CONTRACTORS

Aerospace Corp
ATTN: I. Garfunkel
ATTN: S. Bower
ATTN: D. Olsen
ATTN: N. Stockwell
ATTN: R. Slaughter
ATTN: V. Josephson
ATTN: T. Salmi
ATTN: J. Straus

University of Alaska
ATTN: T. Davis
ATTN: N. Brown
ATTN: Technical Library

Analytical Systems Engineering Corp
ATTN: Radio Sciences

Analytical Systems Engineering Corp
ATTN: Security

DEPARTMENT OF DEFENSE CONTRACTORS (Continued)

Barry Research Corporation
ATTN: J. McLaughlin

BDM Corp
ATTN: L. Jacobs
ATTN: T. Neighbors

Berkeley Research Associates, Inc
ATTN: J. Workman

Betac
ATTN: J. Hirsch

Boeing Co
ATTN: M/S 42-33, J. Kennedy
ATTN: G. Hall
ATTN: S. Tashird

Booz-Allen & Hamilton, Inc
ATTN: B. Wilkinson

University of California at San Diego
ATTN: H. Booker

Charles Stark Draper Lab, Inc
ATTN: D. Cox
ATTN: J. Gilmore

Communications Satellite Corp
ATTN: D. Fang

COMSAT Labs
ATTN: R. Taur
ATTN: G. Hyde

Cornell University
ATTN: M. Kelly
ATTN: D. Farley, Jr

Electrospace Systems, Inc
ATTN: H. Logston

ESL, Inc
ATTN: J. Marshall

General Electric Co
ATTN: M. Bortner
ATTN: A. Harcar

General Electric Co
ATTN: A. Steinmayer
ATTN: C. Zierdt

General Electric Co
ATTN: F. Reibert

General Electric Tech Services Co, Inc
ATTN: G. Millman

General Research Corp
ATTN: J. Ise, Jr
ATTN: J. Garbarino

Harris Corp
ATTN: E. Knick

Horizons Technology, Inc
ATTN: R. Kruger

DEPARTMENT OF DEFENSE CONTRACTORS (Continued)

HSS, Inc
ATTN: D. Hansen

IBM Corp
ATTN: F. Ricci

University of Illinois
ATTN: Security Supervisor for K. Yeh

Institute for Defense Analyses
ATTN: J. Bengston
ATTN: E. Bauer
ATTN: H. Wolfhard
ATTN: J. Aein

International Tel & Telegraph Corp
ATTN: G. Wetmore
ATTN: Technical Library

JAYCOR
ATTN: J. Sperling

JAYCOR
ATTN: J. Doncarlos

Johns Hopkins University
ATTN: T. Potemra
ATTN: J. Phillips
ATTN: T. Evans
ATTN: J. Newland
ATTN: P. Komiske

Kaman Tempo
ATTN: DASIAC
ATTN: W. McNamara
ATTN: T. Stephens
ATTN: W. Knapp

Linkabit Corp
ATTN: I. Jacobs

Litton Systems, Inc
ATTN: R. Grasty

Lockheed Missiles & Space Co, Inc
ATTN: W. Imhof
ATTN: M. Walt
ATTN: R. Johnson

Lockheed Missiles & Space Co, Inc
ATTN: Dept 60-12

M.I.T. Lincoln Lab
ATTN: D. Towle

Martin Marietta Corp
ATTN: R. Heffner

McDonnell Douglas Corp
ATTN: G. Mroz
ATTN: N. Harris
ATTN: W. Olson
ATTN: J. Moule
ATTN: R. Halprin

Meteor Communications Consultants
ATTN: R. Leader

DEPARTMENT OF DEFENSE CONTRACTORS (Continued)

Mission Reserach Corp
ATTN: R. Kilb
ATTN: R. Bogusch
ATTN: D. Sappenfield
ATTN: F. Fajen
ATTN: R. Hendrick
ATTN: S. Gutsche
ATTN: Tech Library

Mitre Corp
ATTN: G. Harding
ATTN: A. Kymmel
ATTN: B. Adams
ATTN: C. Callahan

Mitre Corp
ATTN: M. Horrocks
ATTN: J. Wheeler
ATTN: W. Foster
ATTN: W. Hall

Pacific-Sierra Research Corp
ATTN: E. Field, Jr
ATTN: F. Thomas
ATTN: H. Brode

Pennsylvania State University
ATTN: Ionospheric Research Lab

Photometrics, Inc
ATTN: I. Kofsky

Physical Dynamics, Inc
ATTN: E. Fremouw

Physical Research, Inc
ATTN: R. Deliberis

R & D Associates
ATTN: R. Turco
ATTN: C. Greifinger
ATTN: M. Gantsweg
ATTN: B. Gabbard
ATTN: W. Wright
ATTN: R. Lelevier
ATTN: F. Gilmore
ATTN: W. Karzas
ATTN: H. Ory
ATTN: P. Haas

R & D Associates
ATTN: B. Yoon

Rand Corp
ATTN: C. Crain
ATTN: E. Bedrozian

Riverside Research Institute
ATTN: V. Trapani

DEPARTMENT OF DEFENSE CONTRACTORS (Continued)

Rockwell International Corp
ATTN: R. Buckner

Rockwell International Corp
ATTN: S. Quilici

Santa Fe Corp
ATTN: D. Paolucci

Science Applications, Inc
ATTN: C. Smith
ATTN: D. Hamlin
ATTN: E. Straker
ATTN: L. Linson

Science Applications, Inc
ATTN: SZ

Science Applications, Inc
ATTN: J. Cockayne

SRI International
ATTN: W. Jaye
ATTN: R. Leadabrand
ATTN: D. Neilson
ATTN: J. Petrickes
ATTN: W. Chesnut
ATTN: R. Livingston
ATTN: R. Tsunoda
ATTN: G. Smith
ATTN: G. Price
ATTN: M. Baron
ATTN: A. Burns
4 cy ATTN: C. Rino

Sylvania Systems Group
ATTN: M. Cross

Technology International Corp
ATTN: W. Boquist

TRI-COM, Inc
ATTN: D. Murray

TRW Defense & Space Sys Group
ATTN: D. Dee
ATTN: R. Plebuch

Utah State University
ATTN: L. Jensen
ATTN: J. Dupnik
ATTN: K. Baker

Visidyne, Inc
ATTN: C. Humphrey
ATTN: J. Carpenter

DATE
ILMED
-8